

## **Supplementary Information**

### **Transcranial contrast-enhanced ultrasound in the rat brain reveals substantial hyperperfusion acutely post-stroke**

Dino Premilovac<sup>1</sup>, Sarah J. Blackwood<sup>2</sup>, Ciaran J. Ramsay<sup>1</sup>, Michelle A. Keske<sup>3</sup>, David W. Howells<sup>1</sup> and Brad A. Sutherland<sup>1</sup>

<sup>1</sup> School of Medicine, College of Health and Medicine, University of Tasmania, Hobart, Tasmania, Australia

<sup>2</sup> Åstrand Laboratory of Work Physiology, Swedish School of Sport and Health Sciences, GIH, Stockholm, Sweden

<sup>3</sup> Institute for Physical Activity and Nutrition (IPAN), School of Exercise and Nutrition Sciences, Deakin University, Geelong, Victoria, Australia.

**Running title:** Cerebral perfusion with CEU during stroke

#### **Corresponding Author:**

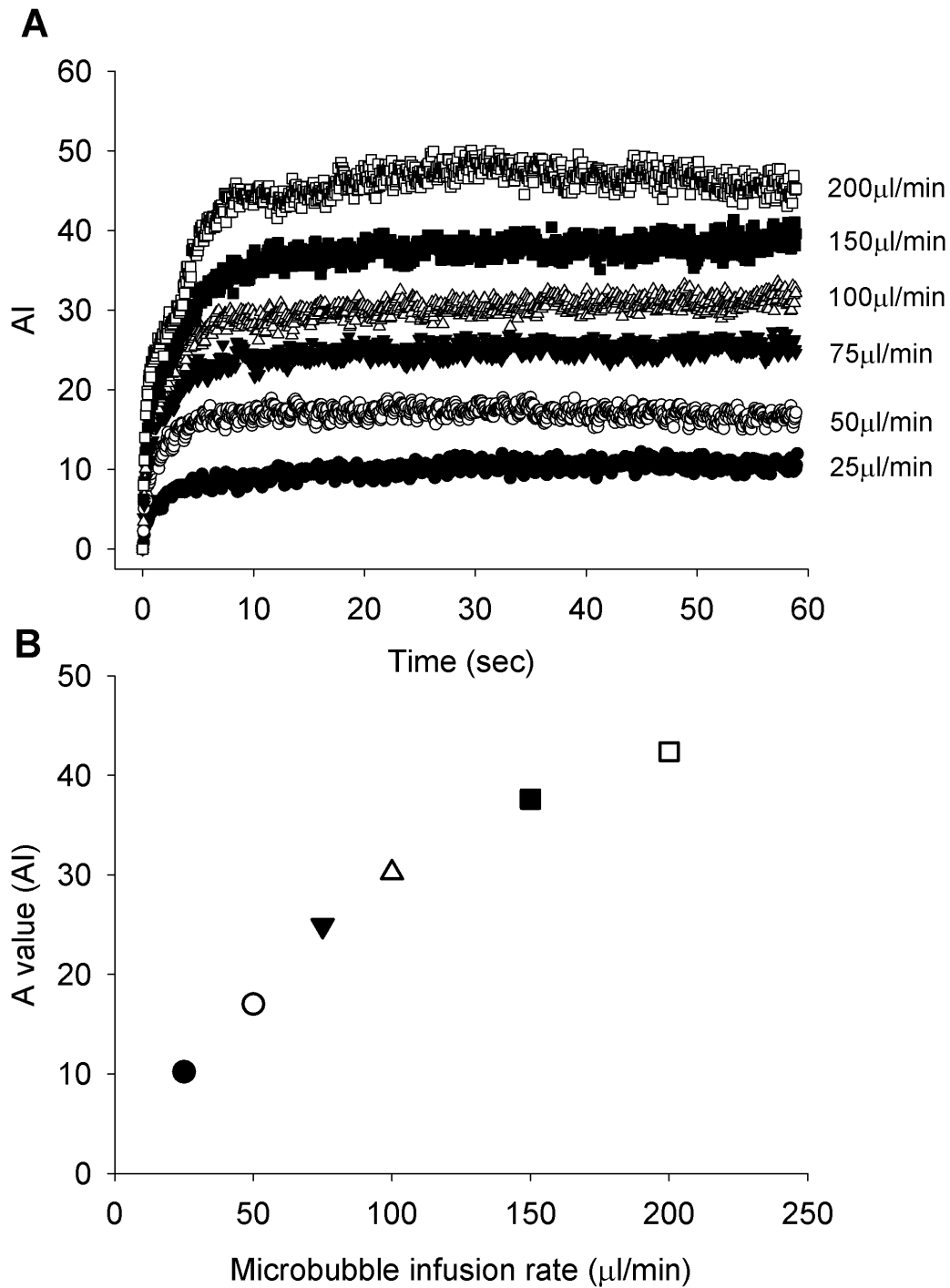
Brad A. Sutherland (PhD)

School of Medicine, College of Health and Medicine, University of Tasmania

Hobart, TAS 7000, Australia

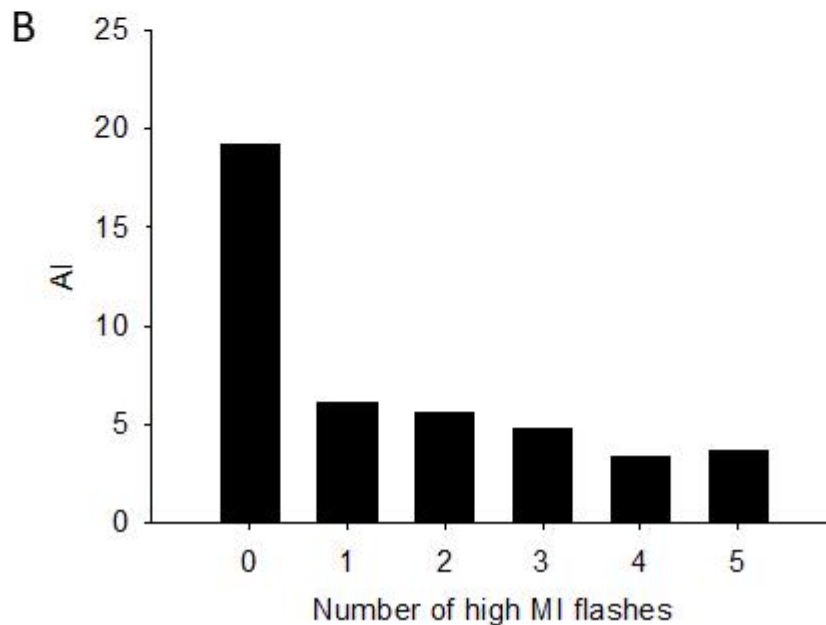
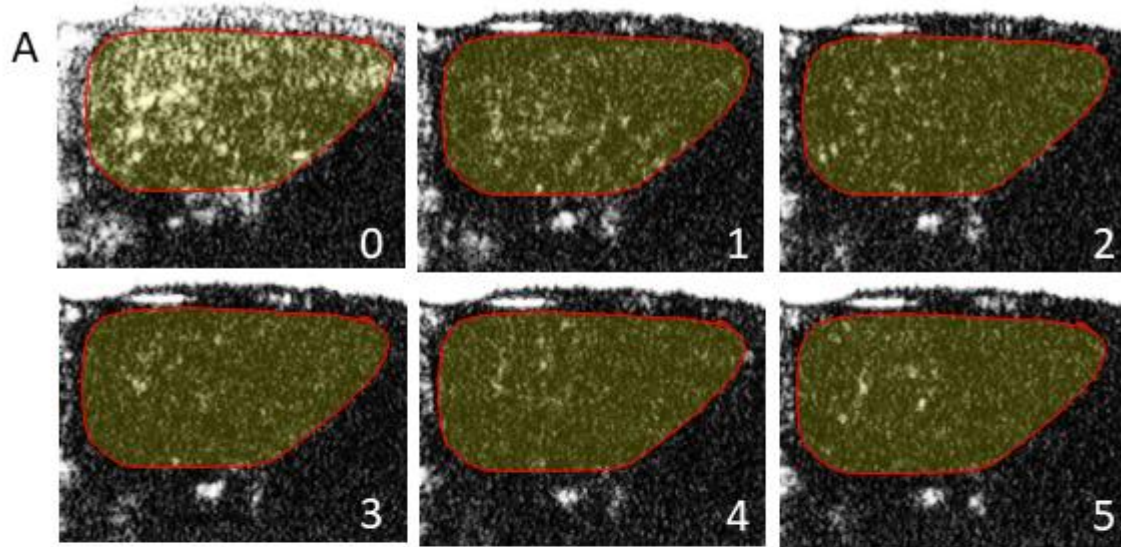
P: +613 6226 7634

[brad.sutherland@utas.edu.au](mailto:brad.sutherland@utas.edu.au)



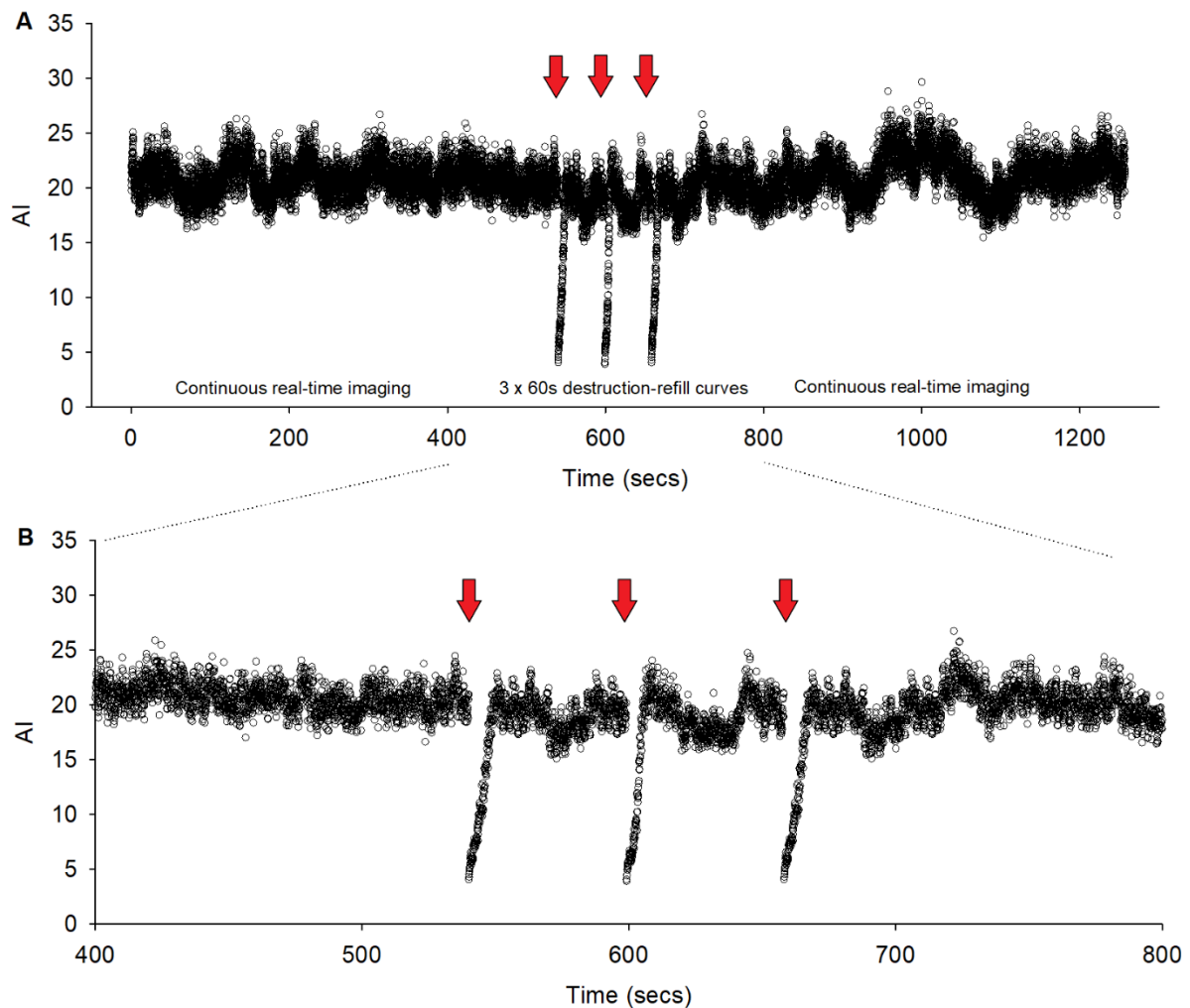
**Supplementary Figure 1. Optimisation of microbubble dose-response relationship using transcranial CEU.** A single rat was used, and an intravenous cannula inserted into a branch of the right jugular vein. The ultrasound transducer was positioned above the rat's head as outlined in Figure 1. **(A)** Microbubbles were infused at the rates indicated, beginning at 25µl/min and increasing sequentially to 200µl/min.

Microbubbles were infused for three minutes at each infusion rate to ensure constant arterial saturation prior to performing 60 second destruction-refill imaging. **(B)** The A values (representing blood volume) calculated from each infusion rate were plotted against infusion rate to produce the microbubbles dose-response curve using transcranial CEU.



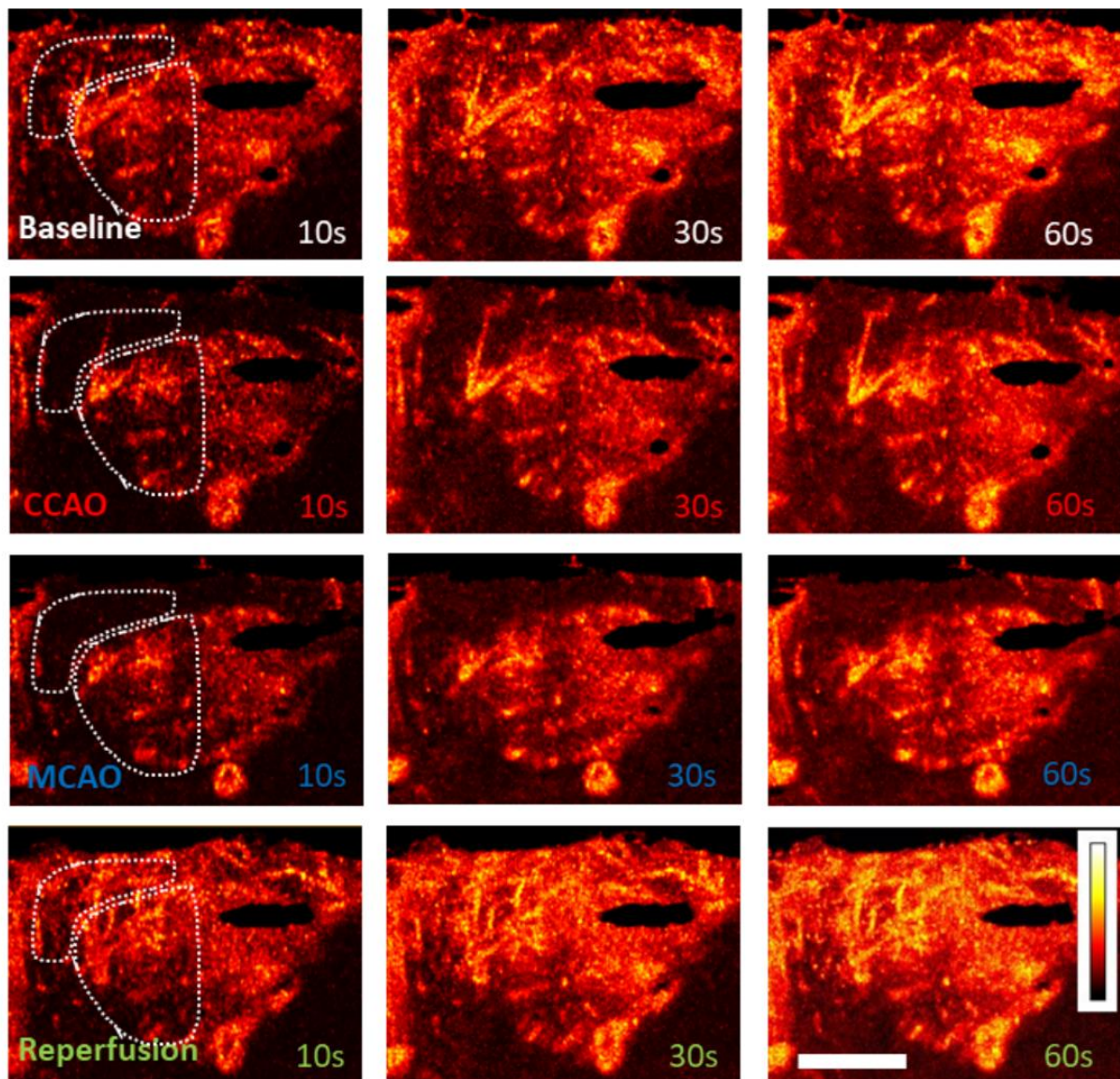
**Supplementary Figure 2. Optimisation of high mechanical index ultrasound flashes to destroy microbubbles.** A single rat was used, and an intravenous cannula inserted into a branch of the right jugular vein. The ultrasound transducer was positioned above the rat's head as outlined in Figure 1. **(A)** Microbubbles were infused and low mechanical index ( $MI = 0.24$ ) ultrasound was used to image the acoustic intensity of the brain. Increasing numbers of high MI ( $1.20$ ) flashes were used to destroy the microbubbles with low MI imaging occurring immediately after to detect

acoustic intensity. The images show a gradual decrease in acoustic intensity signal with increasing number of pulses. **(B)** Quantification of acoustic intensity in the brain showing a greater depletion of microbubbles with increased number of high MI flashes.



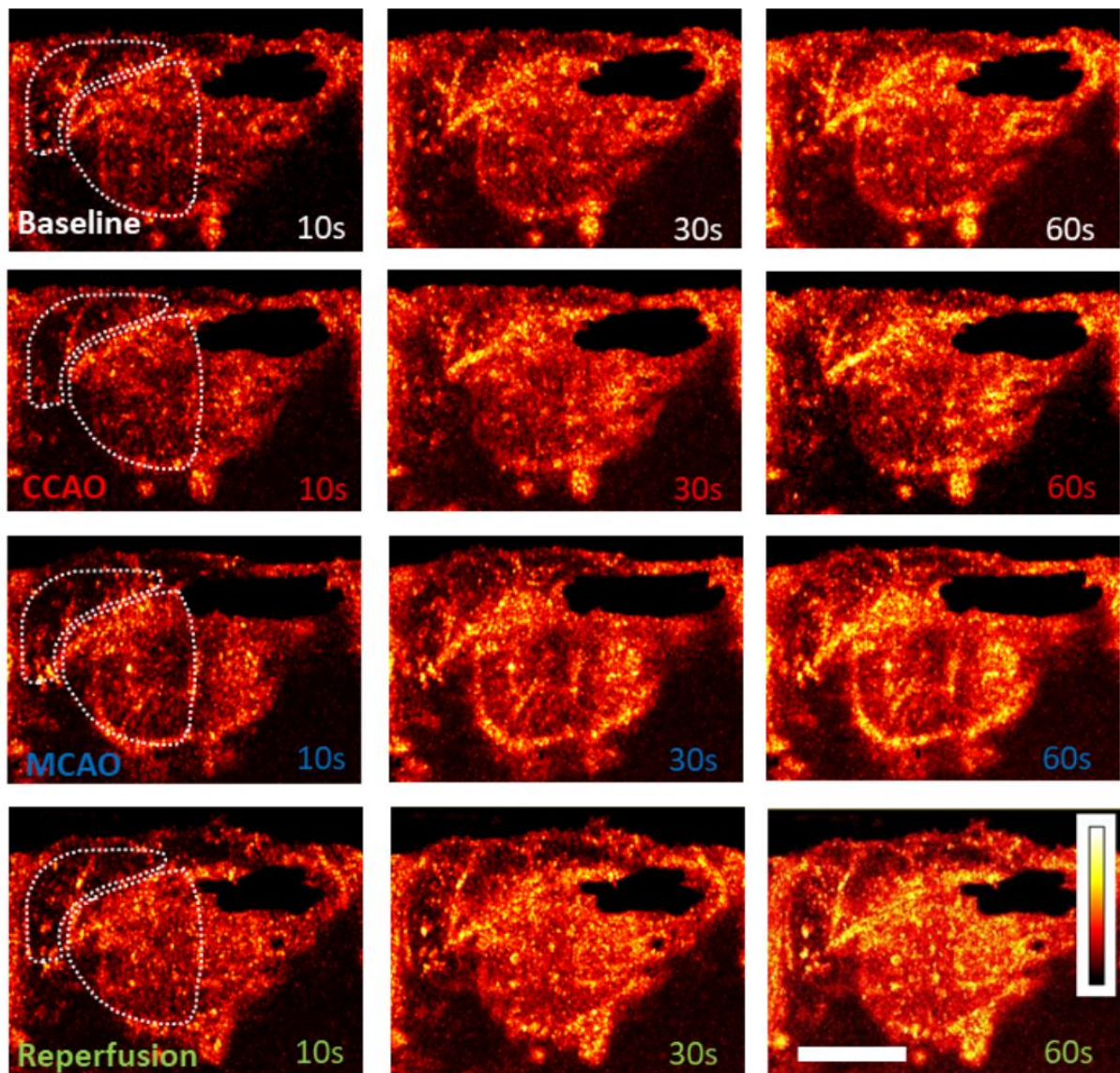
**Supplementary Figure 3. Assessing changes in acoustic intensity (AI) following repeated destruction refill kinetics.** Transcranial CEU was performed on one animal to assess how repeated destruction-refill imaging affected the plateau position of AI. Microbubbles were infused at 50 $\mu$ l/min for twenty-one minutes and real-time, continuous low MI (0.24) imaging was used to assess the cerebral blood flow over the first nine minutes. After nine minutes, high MI (1.20; red arrow) ultrasound was used to clear the underlying vasculature of microbubbles after which continuous low MI imaging was used to assess refill kinetics back into the cerebral vasculature over 60 seconds. This process was repeated three times and shows that the microbubbles signal reaches the plateau position within the 60 second destruction-refill measure.

Continuous low MI (0.24) imaging over the following nine minutes showed that even after microbubbles were destroyed, the acoustic intensity returned to baseline levels and the levels of vasomotion were not affected by the repeated high MI pulses.

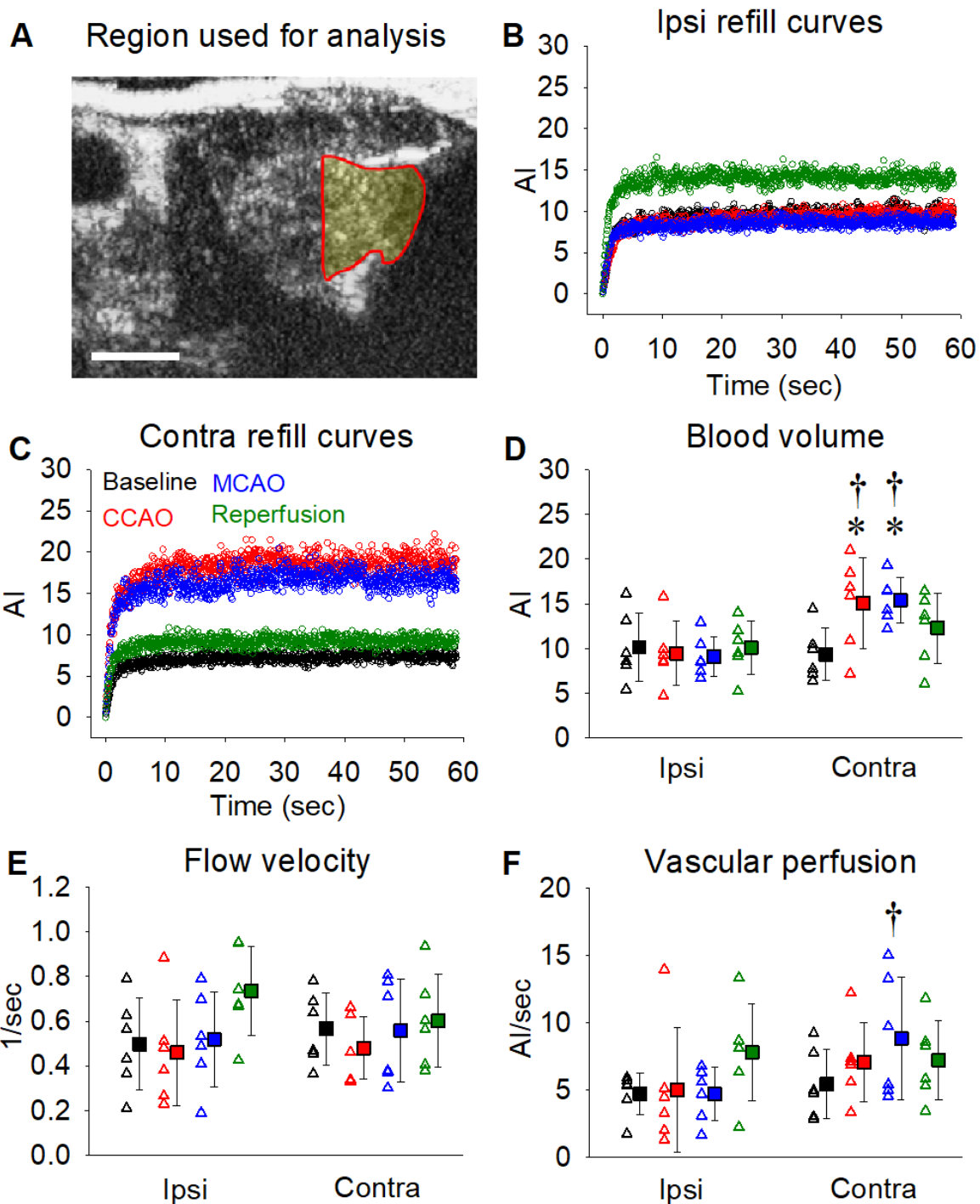


**Supplementary Figure 4. Tracking blood flow distribution in the ipsilateral cerebral vasculature before, during and after MCAO using microvascular imaging (MVI).** Representative MVI images from the ipsilateral hemisphere (MCAO) are shown from one animal 10, 30 and 60 seconds following a destructive ultrasound pulse for baseline, common carotid artery occlusion (CCA0), middle cerebral artery occlusion (MCAO) and reperfusion. Images were generated using the MVI function in QLAB software from one of the 60 second destruction refill curves performed at each time point and converted into heat-intensity maps using Image J. Both the cortex and striatum are outlined. Scale bar = 0.5cm.



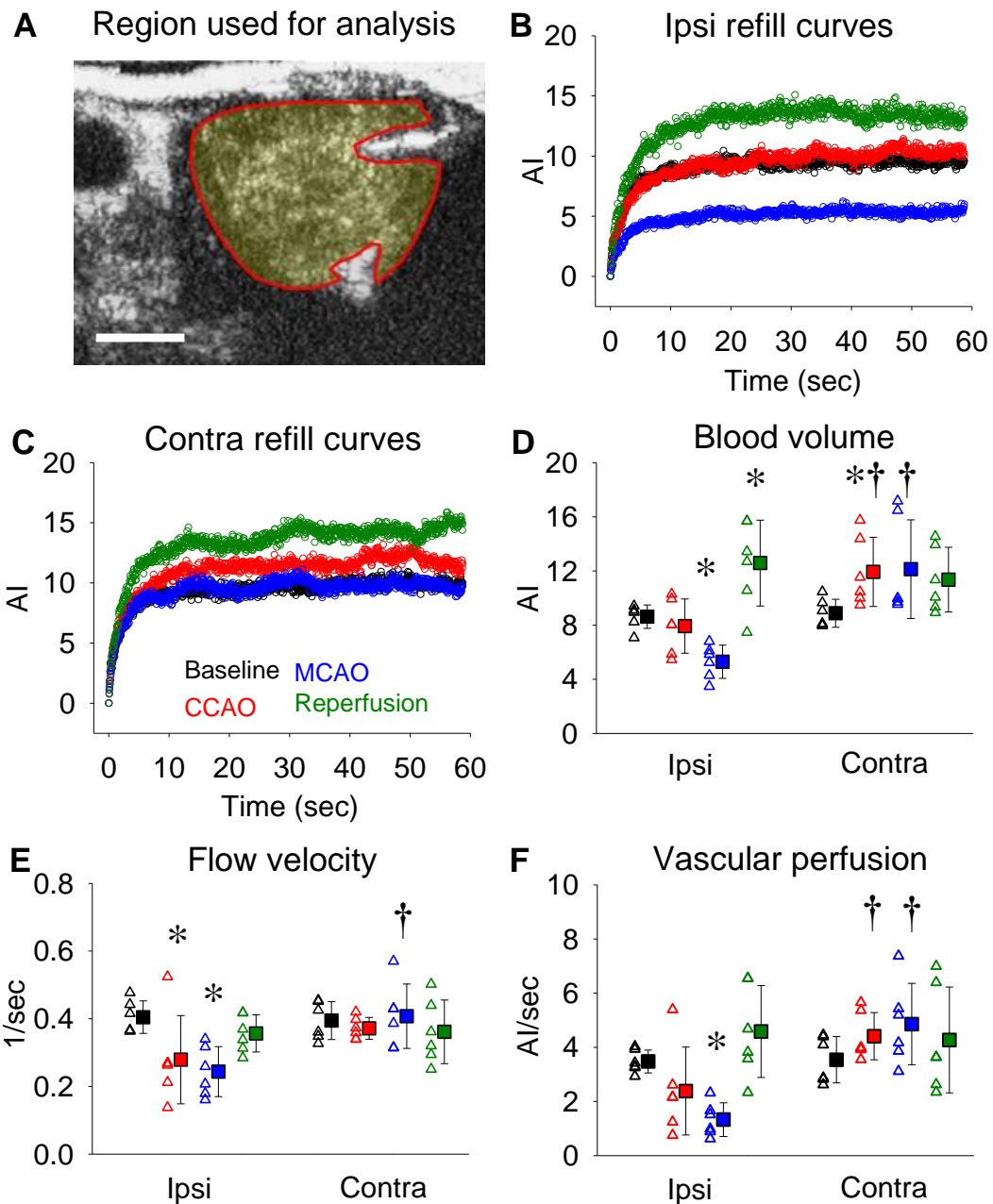


**Supplementary Figure 5. Tracking blood flow distribution in the contralateral cerebral vasculature before, during and after MCAO using microvascular imaging (MVI).** Representative MVI images from the contralateral hemisphere (no MCAO) are shown from one animal 10, 30 and 60 seconds following a destructive ultrasound pulse for baseline, common carotid artery occlusion (CCAO), middle cerebral artery occlusion (MCAO) and reperfusion. Images were generated using the MVI function in QLAB software from one of the 60 second destruction refill curves performed at each time point and converted into heat-intensity maps using Image J. Both the cortex and striatum are outlined. Scale bar = 0.5cm.



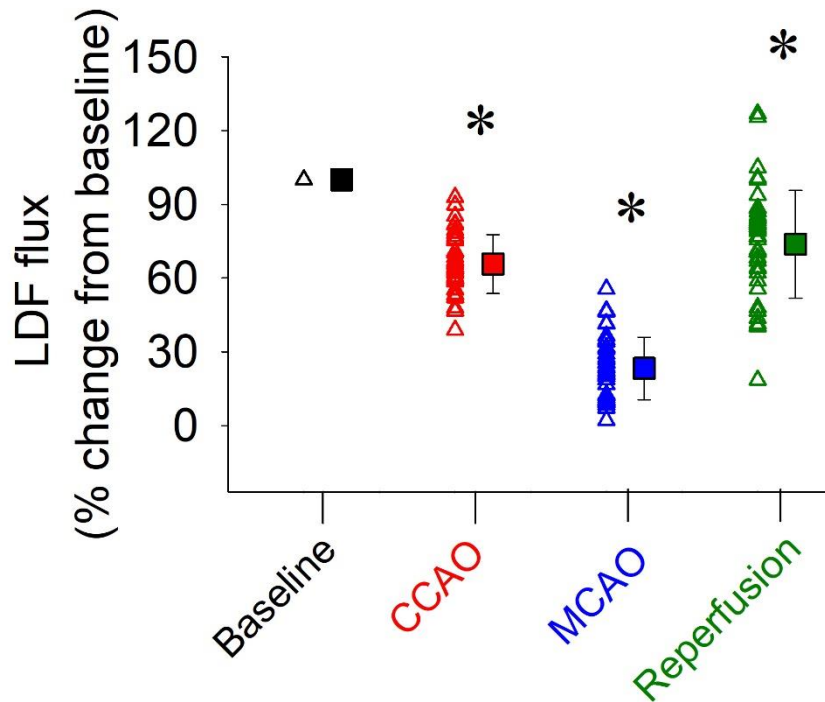
**Supplementary Figure 6. Posterior sub-cortical blood volume increases in the contralateral hemisphere during MCAO.** The region of interest used to quantify blood flow changes in the posterior sub-cortical area is shown in panel (A). Representative 60 second destruction-refill curves from one animal for each of the time-points (baseline, CCAO, MCAO and reperfusion) are shown for the ipsilateral

hemisphere (**B**) and contralateral hemisphere (**C**). Blood volume (**D**), flow velocity (**E**) and vascular perfusion (**F**) were calculated for each time-point across both ipsilateral and contralateral hemispheres as outlined in figure 1d. Open triangles represent individual values from independent experiments and filled squares represent the means  $\pm$  SD for 6 rats. \* denotes  $p < 0.05$  vs within group baseline, † denotes  $p < 0.05$  vs ipsilateral at the same time-point as assessed by repeated measures two-way ANOVA with SNK post-hoc. Scale bar = 0.5cm.



**Supplementary Figure 7. Whole hemisphere blood volume, flow velocity and vascular perfusion are decreased during MCAO.** The region of interest used to quantify blood flow changes across the whole hemisphere is shown in panel (A). Representative 60 second destruction-refill curves from one animal for each of the time-points (baseline, CCAO, MCAO and reperfusion) are shown for the ipsilateral hemisphere (B) and contralateral hemisphere (C). Blood volume (D), flow velocity (E) and vascular perfusion (F) were calculated for each time-point across both ipsilateral

and contralateral hemispheres as outlined in figure 1d. Open triangles represent individual values from independent experiments and filled squares represent the means  $\pm$  SD for 6 rats. \* denotes  $p < 0.05$  vs within group baseline, † denotes  $p < 0.05$  vs ipsilateral at the same time-point as assessed by repeated measures two-way ANOVA with SNK post-hoc. Scale bar = 0.5cm.



**Supplementary Figure 8. Cerebral blood flow is reduced following CCAO and MCAO as measured by Laser Doppler Flowmetry (LDF).** Cerebral blood flow as measured by LDF in male Wistar rats that underwent the transient intraluminal filament model of MCAO for 90 mins. As part of the surgery to achieve MCAO, the common carotid artery also becomes occluded (CCAO). Filament retraction led to reperfusion. These data are from a historical cohort of rats (n=44), the methods are described in Sutherland & Buchan 2013 (ref 4 in main manuscript) and is the same model as used in the current manuscript. LDF data are normalized to baseline (100%). Open triangles represent individual values from independent experiments and filled squares represent the means  $\pm$  SD for 44 rats. \* denotes  $p < 0.05$  vs within group baseline as assessed by repeated measures one-way ANOVA.

**Supplementary video 1.** Representative real-time CEU movie from a single experiment demonstrating microbubble refill kinetics at baseline over the first 10 seconds following a burst of high intensity ultrasound destruction in the ipsilateral hemisphere.

**Supplementary video 2.** Representative real-time CEU movie from a single experiment demonstrating microbubble refill kinetics at CCAO over the first 10 seconds following a burst of high intensity ultrasound destruction in the ipsilateral hemisphere.

**Supplementary video 3.** Representative real-time CEU movie from a single experiment demonstrating microbubble refill kinetics at MCAO over the first 10 seconds following a burst of high intensity ultrasound destruction in the ipsilateral hemisphere.

**Supplementary video 4.** Representative real-time CEU movie from a single experiment demonstrating microbubble refill kinetics at Reperfusion over the first 10 seconds following a burst of high intensity ultrasound destruction in the ipsilateral hemisphere.

**Supplementary video 5.** Representative movie demonstrating the use of the microvascular imaging (MVI) function to track blood flow distribution in the cerebral vasculature over the 5 seconds following a burst of high intensity ultrasound.